Fire Technology, 57, 683–697, 2021

Manufactured in The United States
https://doi.org/10.1007/s10694-020-01018-5

Investigating Coupled Effect of Radiative Heat Flux and Firebrand Showers on Ignition of Fuel Beds

*Sayaka Suzuki, National Research Institute of Fire and Disaster (NRIFD), Chofu, Tokyo 182-8508, Japan

Samuel L. Manzello, National Institute of Standards and Technology (NIST), Gaithersburg, MD 20899-8665, USA

Received: 21 May 2020/**Accepted:** 7 July 2020

Abstract. Fire spread occurs via radiation, flame contact, and firebrands. While firebrand showers are known to be a cause of spot fires which ignite fuels far from the main fire front, in the case of short distance spot fires, radiation from the main fire may play a role for firebrand induced ignition processes. Many past investigations have focused on singular effects on fire spread, and little is known about coupled effects. The coupled effect of radiative heat flux and firebrand showers on ignition processes of fuel beds is studied by using a newly developed experimental protocol. The newly developed protocol includes the addition of a radiant panel to the existing experimental setup of a firebrand generator coupled to a wind facility. Experiments were performed under an applied wind field, as the wind is a key parameter in large outdoor fire spread processes. Results show that radiant heat flux plays an important role for ignition by firebrands under 6 m/s while little effect was observed under 8 m/s.

Keywords: Firebrands, Ignition, Radiation, Large outdoor fires, WUI fires, Urban fires

1. Introduction

Large outdoor fires pose problems for societies across the world [1, 2]. Perhaps the most often in the news are wildland fires that approach urban areas. These are more simply referred to as Wildland-Urban Interface (WUI) fires [3]. In Asia and North America, some recent examples are the 2019 WUI fires that occurred in South Korea and those in 2018 in Northern California in the United States [4–6]. In Africa, in less developed countries, there have been large fires that have occurred in informal settlements [7]. For centuries there have also been large urban fires in Japan, a country with no large wildland fire problem or informal settlement situation [2].

In all of these large outdoor fires, fires spread in three mechanisms: direct flame contact, thermal radiation, and firebrands as shown in Fig. 1. Firebrands are pro-

* Correspondence should be addressed to: Sayaka Suzuki, E-mail: sayakas@fri.go.jp

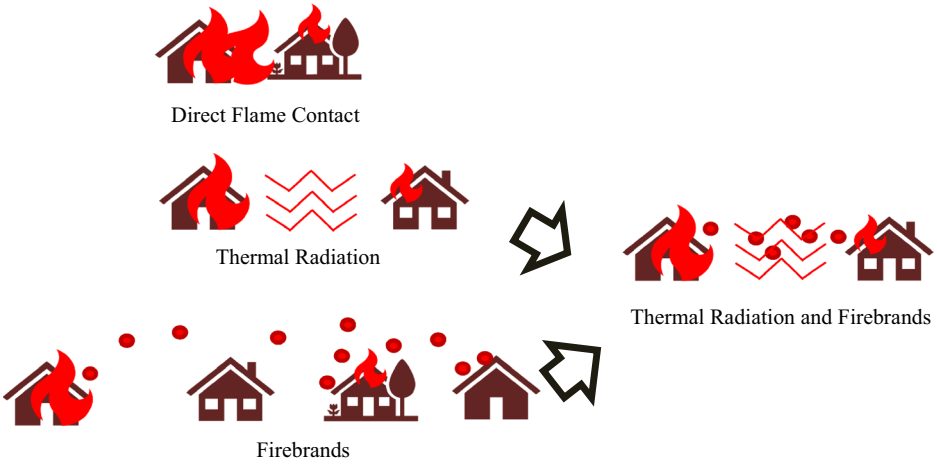

Figure 1. Fire spread mechanisms in large outdoor fires: direct flame contact, thermal radiation and firebrands.

duced and lead to enhanced fire spread processes [8–27]. Often referred to as spotting processes, firebrands are liberated from the combustion of various fuel types, such as trees, shrubs, houses, and then induce ignition of fuel sources away from the initial fire source. In the case of short distance spot fires (distance up to 500 m to 750 m [28]), a potentially important aspect of the physics of ignition induced by firebrand are the coupled influence of firebrand showers and radiant heat. Many past investigations have focused on singular effects on fire spread [11, 23–27], and little is known about coupled effects.

Here, the coupled effect of radiation and firebrand showers on ignition processes of fuel beds is studied by using a newly developed experimental protocol. Experiments were performed under an applied wind field, as the wind is a key parameter in large outdoor fire spread processes.

2. Experimental Description

All experiments were conducted at the National Research Institute of Fire and Disaster (NRIFD). The wind field exits from a 4.0 m diameter fan, and it is possible to generate wind speeds up to 10 m/s. The flow field was measured to be within $\pm$ 10% of desired wind speed over a cross-section of 2.0 m by 2.0 m. To generate firebrand showers, the reduced-scale continuous-feed firebrand generator was used and installed inside NRIFD's wind facility [29]. This apparatus is known to have the ability to produce firebrand showers often seen in actual large outdoor fires (Fig. 2). Figure 2 offers comparison of firebrands in actual WUI fires [30] and firebrands from the firebrand generator. The experimental facility was modified for this work with the new aspect being the addition of a radiant panel to provide radiant heat to the fuel beds.

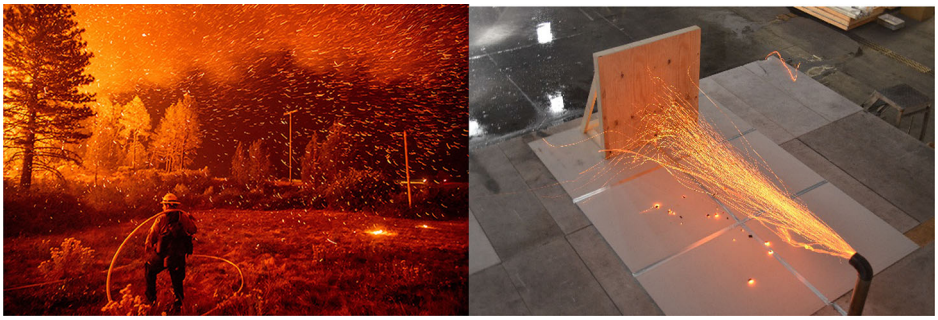

Figure 2. Comparison of firebrands in WUI fires (left) and firebrands from a firebrand generator under a 4 m/s wind (right). Image in left is from [30] showing WUI fires in California, USA 2018.

2.1. Experimental Apparatus

The reduced-scale continuous-feed firebrand generator consisted of two parts: the main body where combustion takes place and continuous feeding component (see Fig. 3). A conveyer was used to feed wood pieces continuously into the device and was operated at 1.0 cm/s, and wood pieces were put on the conveyer belt at 12.5 cm intervals. Douglas-fir wood pieces machined with dimensions of 7.9 mm (H) by 7.9 mm (W) by 12.7 mm (L) were used to produce firebrands. These same size wood pieces were used in past studies and have been shown to be within the projected area and the mass of firebrands measured from full-scale burning trees as projected areas obtained from actual WUI fires [31]. The wood feed rate used here was 80 g/min (mass based) or 160/min (number based), similar to previous non-radiation assisted ignition studies [29]. As glowing firebrands were desired, the blower was set to provide an average velocity of 500 cm/s.

The fuel beds used for ignition were 300 mm by 300 mm in size and consisted of the same Douglas-fir wood pieces used to generate firebrands (Fig. 4a, b). These were installed inside a mock-up corner assembly lined with calcium silicate board, since the ignition of the corner assembly itself was not the goal here; only ignition induced in the wood pieces was of interest. It was observed that firebrands deposited uniformly on the fuel beds when installed inside the mock-up corner assembly. To further simplify the experiments, these wood pieces in the fuel beds were oven dried to remove moisture at 104°C. Moisture removal was verified by measuring the temporal variation of mass loss of the wood pieces.

To provide uniform radiant heat flux to fuel beds, an electrically operated quartz radiant panel was used. Dimensions of the radiant panel were also 300 mm by 300 mm (Fig. 4a, b). It was mounted at a height of 440 mm from the fuel bed surface.

2.2. Experimental Condition

The two wind speeds were selected, namely 6 m/s and 8 m/s for this experimental series. The objective of the new experimental setup is to investigate the combined

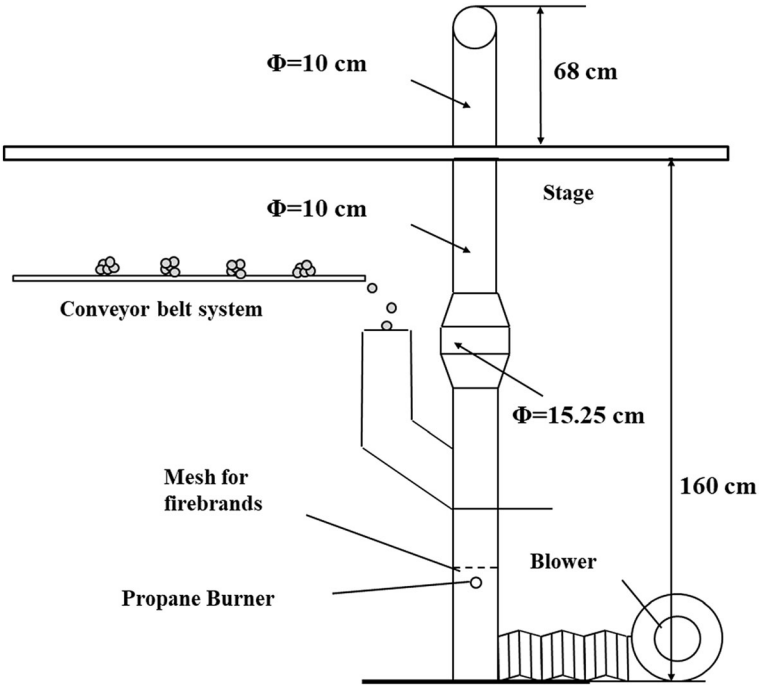

Figure 3. Schematic of a firebrand generator embedded in the wind facility in NRIFD.

effect of radiative heat flux and firebrands on ignition, and therefore the wind speeds were carefully selected. Based on scoping experiments, firebrands are able to ignite fuel beds of wood pieces within 40 min under both wind speeds without radiative heat flux. Firebrand flux landing on fuel bed was measured via video recording (30 frames per second). The firebrand fluxes were $6.3/m^2$ s and $9.0/m^2$ s under 6 m/s and 8 m/s respectively. The characteristics of firebrands, namely the mass and the projected area of firebrands were compared. As shown in Fig. 5, the mass and the projected area of firebrands produced under 6 m/s and 8 m/s wind are similar as those are within similar mass and projected area class and the average within uncertainties.

A custom calibration rig was designed and fabricated to quantify the radiant heat flux that the radiant panel provided at the fuel bed surface. The heat from the radiant panel was 5.76 kW (Quartz-faced Infrared Radiant Panel Heaters, Omega Engineering). The applied radiant heat flux to fuel beds with no wind was $8.5\ kW/m^2$. This value was carefully selected. In this study, it is important to investigate the coupled effects of firebrand showers and radiant heat flux on fuel bed ignition. Naturally, if the radiant heat flux applied to the fuel beds was too high, firebrands would simply serve as piloted ignition source, as the radiant heat flux would be the dominate ignition mode. Accordingly, a series of experiments using only a radiant heater coupled with spark ignitor was undertaken to deter-

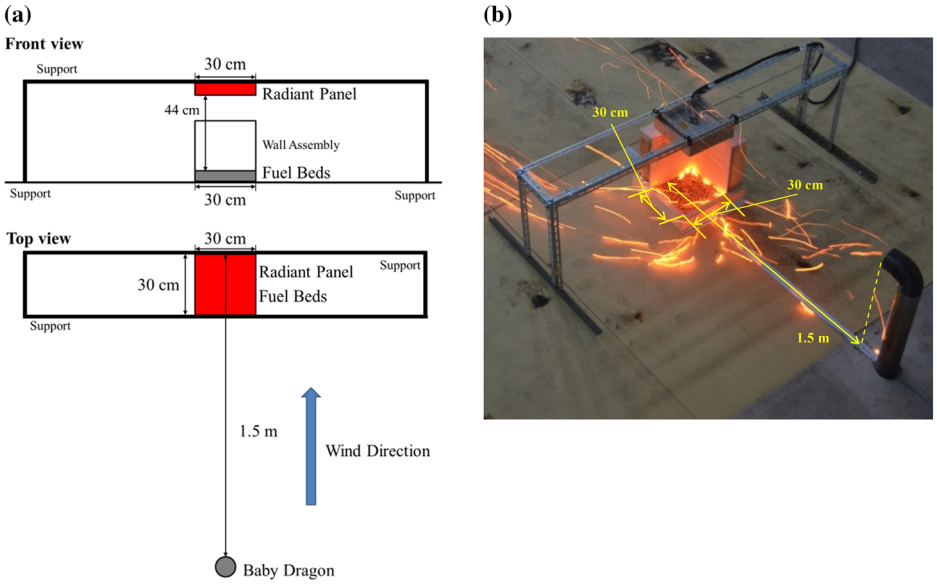

Figure 4. a Schematic of the experimental settings. Front view (top) and Top view (bottom) are shown. Firebrand showers were produced using the reduced-scale firebrand generator installed in NIRFD's wind facility. Fuel beds consisted of Douglas-fir pieces of uniform size. b A typical experiment conducted at 8 m/s. Multiple glowing firebrands are seen depositing in the fuel bed.

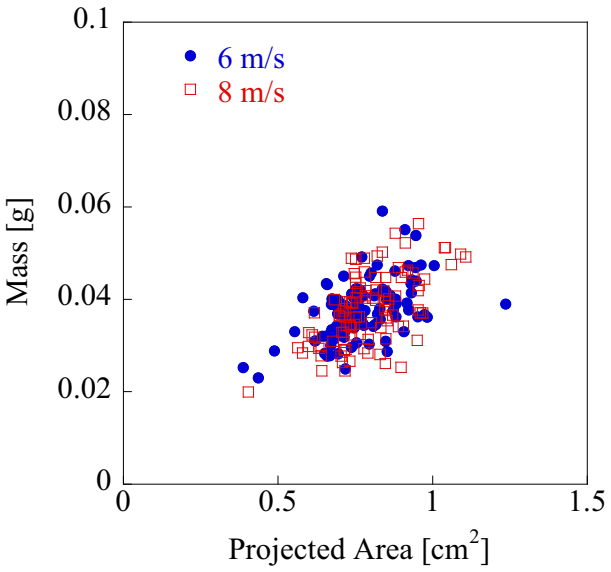

Figure 5. Characteristics of firebrands used in this study.

mine the limits where radiant heat flux alone in the absence of firebrand showers was capable to ignite the fuel beds used here. At 10 kW/m^2, the fuel bed was not able to be ignited by a spark within 30 min. For values above 10 kW/m^2, radiant heat flux in the presence of a spark was able to produce ignition of the fuel beds. The radiant heat was measured at multiple points and found to be within 10%.

The applied wind increases the convective heat loss from the fuel beds, so the measured heat flux to fuel beds, using a total heat flux gauge (Schmidt-Boelter gauge, Hukseflux, calibrated by the manufacturer), under 6 m/s and 8 m/s were 5.6 kW/m^2 and 4.0 kW/m^2, respectively. Pre-heating time was determined as the duration from the time when the radiant panel was turned on to the time to start the firebrand generator. For pre-heating times of 10 min and 20 min, the wind field was switched on 60 s prior to initiating combustion in the firebrand generator. Selected pre-heating time was 0 min, 10 min, and 20 min. Baseline experiments were also performed to examine the ignitions by firebrands without applied radiant heat flux. The experiments for the same condition was repeated at least 3 times.

3. Results and Discussions

Figure 4b displays a picture of a typical experiment. In this picture, the applied wind speed was 8 m/s, and radiant panel was switched on at the same time as the firebrand generator, that is there was no pre-heating time. The experiments for the same condition was repeated at least 3 times, and the uncertainties were calculated based on two standard deviation.

Fig 6 displays the time to smoldering ignition (SI) in the fuel beds a function of pre-heating time and wind speed. As mentioned above, the firebrand flux on the fuel beds differ under 6 m/s and 8 m/s (6.3/m^2 s and 9.0/m^2 s, respectively). The time to ignition did not take into account the difference of firebrand flux, so total number of firebrands per m^2 required is introduced. The total number of firebrands per m^2 required to achieve these ignition sequences is also displayed in Fig. 7. This was calculated by multiplying the time to SI by the firebrand flux. The time to SI was measured via video recording, from the time the first firebrand landed the fuel bed to the time the sustained SI was observed in the fuel bed. Experiments were repeated and the error bars in the figures shows the standard deviation. Here, sustained SI was defined as the start of intense smoke generation and glowing ignition of the fuel bed due to the coupled effects of accumulated firebrands and radiant heat flux. To aid in understanding, in Figs. 6 and 7, no radiant panel conditions denote that the radiant panel was not switched on. For other cases, the applied radiant heat flux to fuel beds was 8.5 kW/m^2.

An interesting result from these findings is that for wind speed of 6 m/s, the pre-heating due to the applied radiant heat flux to the fuel bed influenced the time to SI significantly. Yet, as the wind speed was increased to 8 m/s, the applied radiant heat flux had very little effect.

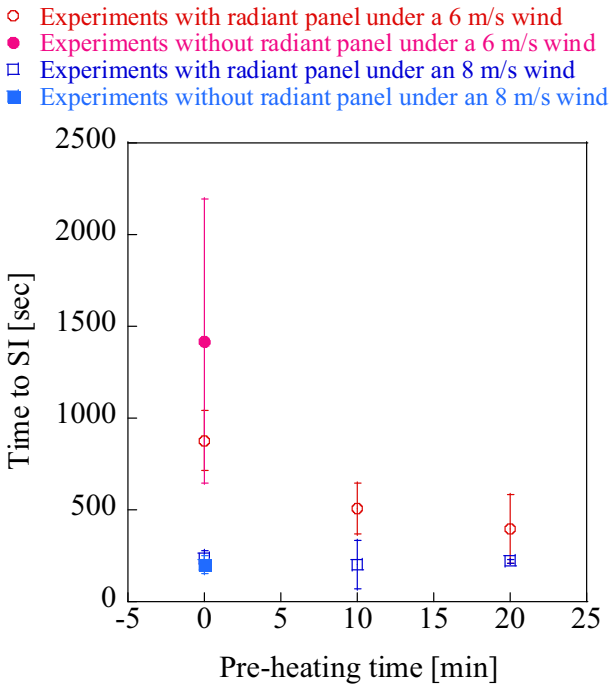

Figure 6. Coupled effects of radiation and firebrands on smoldering ignition under different wind speeds and pre-heating time.

To better visualize these results, it is instrumental to describe the heat and mass transfer processes occurring in the fuel beds and firebrands. Treating the fuel bed and firebrands as a system, an energy balance gives:

$$Q_{fuel,total} = Q_{firebrand,comb} - Q_{firebrand,loss} + Q_{fuel,rad} - Q_{fuel,conv} \tag{1}$$

where $Q_{firebrand,comb}$ is the heat produced from the firebrand combustion, $Q_{firebrand,loss}$ is the convective and radiative heat loss from a firebrand, $Q_{fuel,rad}$ is the external radiant heat provided to the fuel beds, and $Q_{fuel,conv}$ is the convective heat transfer (cooling) to the fuel beds. Since the fuel beds were oven dried in these experiments, the term indicating the energy to remove the fuel bed moisture is omitted.

In order to ignite the fuel beds, $Q_{fuel,total}$ has to be equal to or greater than the heat required for the ignition, Q_{ig}. Assuming ignition occurs when the temperature of the fuel beds reaches the ignition temperature T_{ig}, Q_{ig} may be described as follows:

$$Q_{ig} = \rho_{fuel} c_{fuel} V \left(T_{ig} - T_0\right) \tag{2}$$

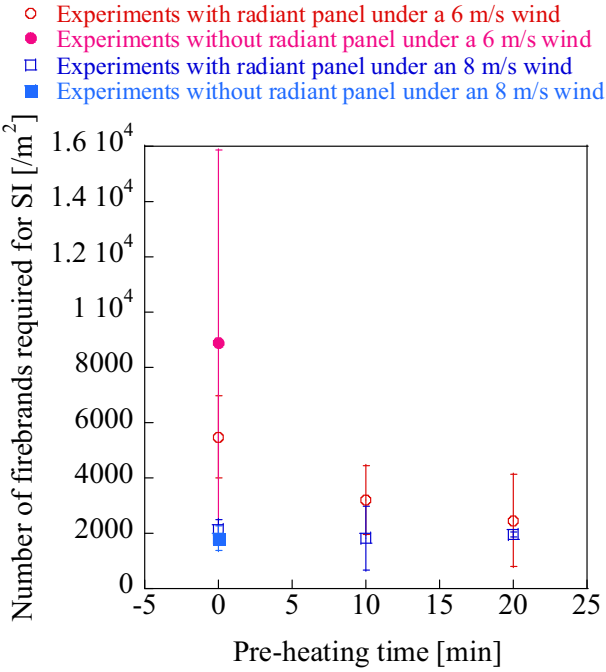

Figure 7. Number of firebrands per m² required for smoldering ignition under different wind speed and pre-heating time.

where ρ_{fuel} is the bulk density of the fuel beds, c_{fuel} is the specific heat capacity of fuel beds (wood), and T_0 is the ambient temperature, and V is volume. $Q_{firebrand,comb}$ is usually described as follows [26]:

$$Q_{firebrand,comb} = \Delta H \times \Delta m_{firebrand} \tag{3}$$

where ΔH is the heat of combustion of a firebrand, and $\Delta m_{firebrand}$ is the mass loss of a given firebrand. The term $Q_{firebrand,loss}$ may be expressed as:

$$Q_{firebrand,\,loss} = \left[h\left(T_{firebrand} - T_0\right) + \epsilon\sigma\left(T_{firebrand}^4 - T_0^4\right)\right] t_{ig} A_{firebrand,\,external} \tag{4}$$

where $A_{firebrand,external}$ is the firebrand area exposed to wind and t_{ig} is the time to fuel bed ignition.

$$\begin{aligned} Q_{fuel,rad} - Q_{fuel,conv} = {} & AERHF\left(t_p + t_0 + t_{ig}\right) A_{fuel,external} \\ & - h\left(T_{fuel} - T_o\right)\left(t_0 + t_{ig}\right) A_{fuel,external} \end{aligned} \tag{5}$$

where AERHF is the applied external radiant heat flux, T_{fuel} is the fuel bed temperature, t_p is the pre-heating time, t_0 is the time when the firebrand generator was on to first firebrand landed on the fuel bed, and $A_{fuel,external}$ is the fuel bed area exposed to wind. Substituting all these expressions into Eq. (1) yields the following:

$$\begin{aligned}\rho_{fuel}c_{fuel}V\left(T_{ig}-T_0\right) = {} & \Delta H \times \Delta m_{firebrand} \\ & - \left[h\left(T_{firebrand}-T_0\right)+\epsilon\sigma\left(T_{firebrand}^4-T_0^4\right)\right]t_{ig}A_{firebrand,external} \\ & + AERHF\left(t_p+t_0+t_{ig}\right)A_{fuel,external} \\ & - h\left(T_{fuel}-T_o\right)\left(t_0+t_{ig}\right)A_{fuel,external}\end{aligned} \tag{6}$$

At 6 m/s, the applied radiant heat flux acts to reduce the time to SI ignition greatly with increased pre-heating time. As wind speed is increased, convection cooling to the fuel beds is increased, but the time to ignition was not influenced by the additional assistance from the applied radiant heat flux. It is believed that the increased wind speed rather changes the combustion dynamics of the firebrands by providing more oxygen and therefore alters their temperatures, resulting in enhanced combustion reactions. There is limited knowledge on the firebrand temperature or heat of combustion of a firebrand [32–34].

Manzello et al. [32] quantitatively showed that glowing firebrand surface temperature increased as the wind speed was increased. As a part of that investigation, the surface temperature of charred area on the glowing firebrand was simultaneously measured using both the thermocouple and the infrared camera [32]. The firebrand temperatures were quite sensitive to airflow. Therefore, in this work, larger firebrand temperatures were expected as the wind speed was increased from 6 m/s to 8 m/s.

Assuming the temperature of a firebrand increases with wind speed, it is known that the final mass of a firebrand under different wind speed decreases with the increasing wind speed [32]. Thus, $Q_{firebrand,comb}$ is expected to increase as the wind speed increases. The temperature increase would result in the increase in $Q_{firebrand,loss}$, assuming t_{ig} is the same. From previous studies [25, 26], it is also known that the t_{ig} becomes shorter as the wind speed increases. In this case, $Q_{firebrand,loss}$ may decrease depending on t_{ig}, cancelling the increase in $Q_{firebrand,loss}$ by temperature increase. The external radiant heat has impact upon the fuel bed ignition. However, the convective cooling and shorter ignition time at a higher wind speed reduces this influence, which is shown in results under 8 m/s.

In every experiment in this investigation, smoldering ignition was observed to transition to flaming ignition. The time to flaming ignition in the fuel beds as function of pre-heating time and wind speed is shown in Fig. 8. The total number of firebrands per m^2 required to reach flaming ignition (FI) was also quantified and shown in Fig. 9.

Fig 10 displays the number of firebrands per m^2 required for ignition versus the calculated total energy per m^2 received at the fuel bed. The total energy received

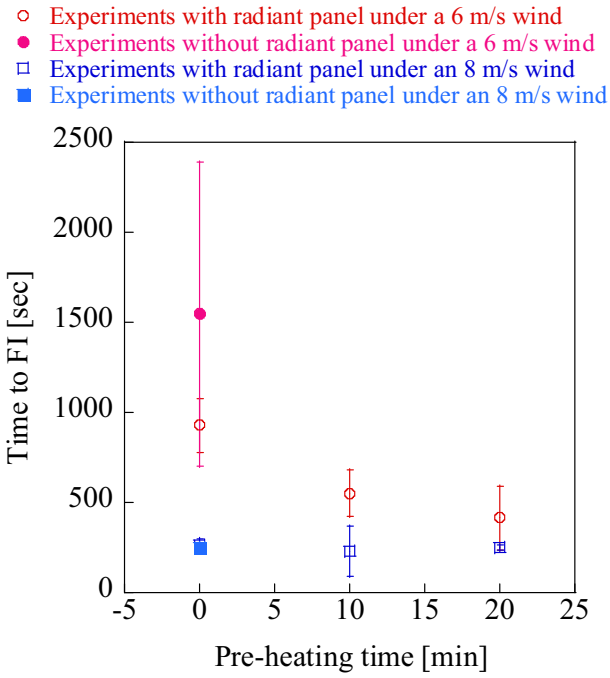

Figure 8. Coupled effects of radiation and firebrands on flaming ignition under different wind speeds and pre-heating time.

at the fuel bed was calculated based on the radiant heat from the radiant panel and the convective heat loss from the fuel bed, the energy from firebrands are not taken into account. Re-writing Eq. (6) as follows yields:

$$\begin{aligned} &-\left[h\left(T_{firebrand}-T_0\right)+\epsilon\sigma\left(T_{firebrand}^4-T_0^4\right)\right]t_{ig}A_{firebrand,external} \\ &+AERHF\left(t_p+t_0+t_{ig}\right)A_{fuel,external}-h\left(T_{fuel}-T_o\right)\left(t_0+t_{ig}\right)A_{fuel,external} \\ &=-\Delta H\times\Delta m_{firebrand}+\rho_{fuel}c_{fuel}V\left(T_{ig}-T_0\right) \end{aligned} \tag{7}$$

where $-\Delta H\times\Delta m_{firebrand}+\rho_{fuel}c_{fuel}V\left(T_{ig}-T_0\right)=constant$, as well as $AERHF\left(t_p+t_0+t_{ig}\right)A_{fuel,external}-h\left(T_{fuel}-T_o\right)\left(t_0+t_{ig}\right)A_{fuel,external}$ can be calculated based on experimental data. The term $-\left[h\left(T_{firebrand}-T_0\right)+\epsilon\sigma\left(T_{firebrand}^4-T_0^4\right)\right]A_{firebrand,external}$ can be considered to be constant under steady conditions. As described above, the number of firebrands per m^2 required for ignition was calculated by multiplying the time to ignition by the firebrand flux. Accordingly, based on these assumptions and calculations, the data in Fig. 10 should follow a linear relationship. As may be seen, data under 6 m/s follows a linear relationship as described in Eq. (7) well. While those under 8 m/s do match the predicted trend, a more detailed heat transfer model of firebrands must be incorporated in the future.

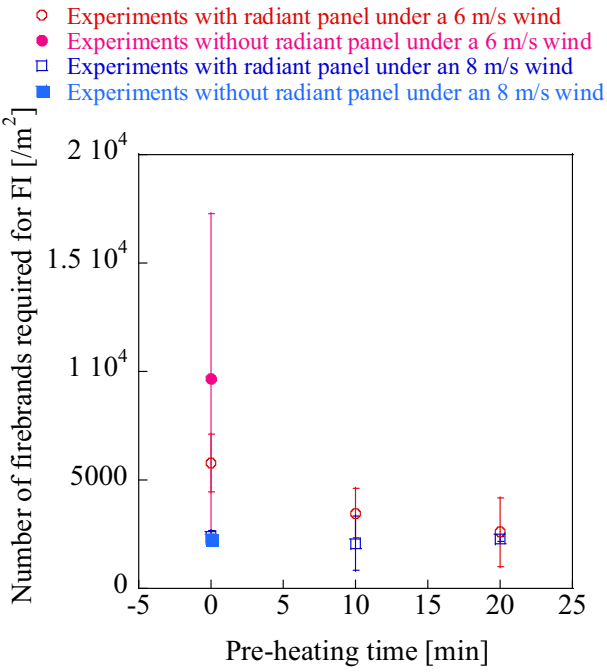

Figure 9. Number of firebrands per m² required for flaming ignition under different wind speed and pre-heating time.

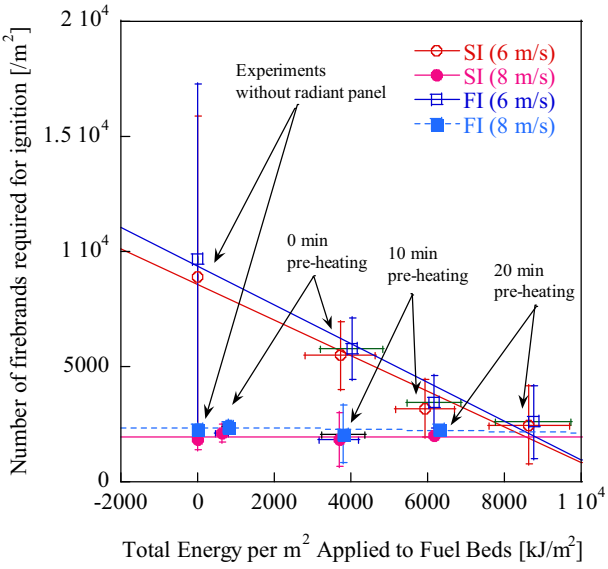

Figure 10. Total received energy per m² to fuel beds and the number of firebrands per m² required for ignition.

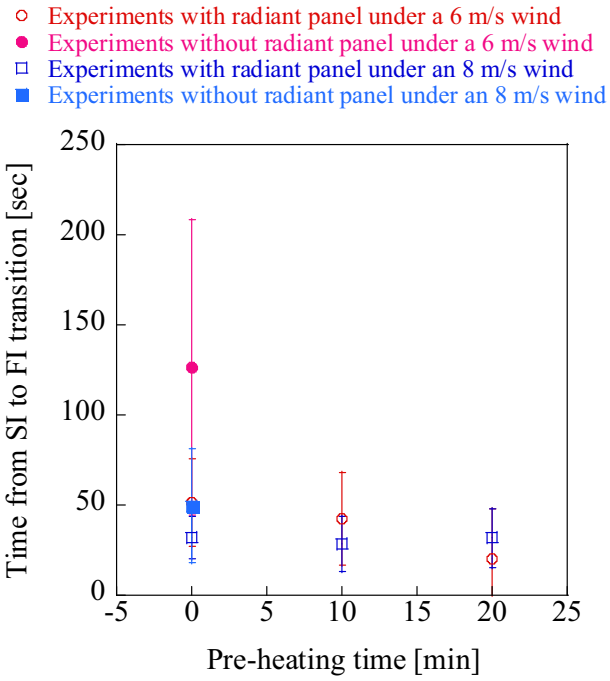

Figure 11. The specific times for transitions from smoldering ignition to flaming were measured and are shown.

The transition to flaming ignition from smoldering ignition is a rapid exothermic gas-phase reaction. For this transition to take place, there are two key events that must be attained simultaneously, a mixture of gases and air within the flammability limit and a sufficient heat source to ignite this mixture [35–37]. It is very interesting to see how these transitions occur under coupled influences of firebrand showers and applied radiant heat. The application of applied radiant heat had the largest influence on the time to reach flaming ignition at 6 m/s. The specific times for these transitions to occur were also measured and shown in Fig. 11, along with the numbers of firebrands required (Fig. 12). For a fixed pre-heat time, additional heat needed to force this transition is provided by the ongoing firebrand showers. While there still exists no complete theory to describe this complex transition [35–37], these experiments provide well-controlled conditions to examine these important processes further.

4. Summary

The coupled effect of radiative heat flux and firebrand showers on ignition processes of fuel beds was studied by using a newly developed experimental protocol. An interesting result from this preliminary study is that for wind speed of 6 m/s, the pre-heating time due to the applied radiant heat flux to the fuel bed influenced

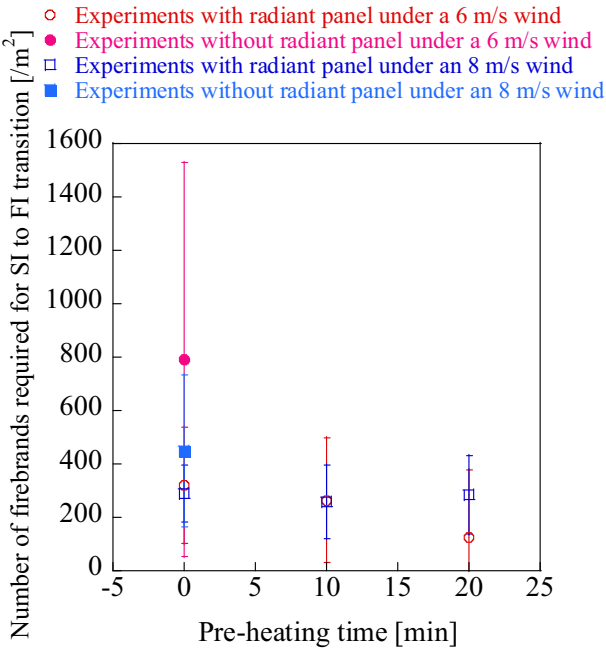

Figure 12. Number of firebrands per m^2 required for transitions from smoldering ignition to flaming ignition under different wind speed and pre-heating time.

the time to SI significantly. Yet, as the wind speed was increased 8 m/s, the applied radiant heat flux had very little effect. It was postulated that differences in firebrand combustion dynamics may explain these differences. More work is required to quantify firebrand temperatures at higher wind speeds. Measurements of firebrand heat of combustion and mass loss profiles would also be important to better reveal the influences of combustion dynamics on applied wind speed.

Acknowledgements

This research is supported by MEXT/JSPS KAKENHI Grant-in-Aid for Scientific Research (C) 18K04675.

Open Access

References

1. Manzello SL, Blanchi R, Gollner MJ, Gorham D, McAllister S, Pastor E, Planas E, Reszka P, Suzuki S (2018) Summary of workshop large outdoor fires and the built environment. Fire Saf J 100:76–92
2. Manzello SL (2019) Summary of workshop on global overview of large outdoor fire standards, NIST special publication (NIST SP)—1235 https://doi.org/10.6028/NIST.SP.1235
3. Mell WE, Manzello SL, Maranghides A, Butry D, Rehm RG (2010) The wildland–urban interface fire problem–current approaches and research needs. Int J Wildl Fire 19(2):238–251
4. Marlon JR et al (2012) Long-term perspective on wildfires in the western USA. Proc Natl Acad Sci 109:E535–E543; https://doi.org/10.1073/pnas.1112839109
5. Thousands Flee South Korea Wildfire, Wildland firefighter. http://www.wildlandfirefighter.com/2019/04/05/thousands-flee-south-korea-wildfire/#gref (2020/July/06 access)
6. CALFIRE 2018 Incident Archives https://www.fire.ca.gov/incidents/2018/ (2020/July/06 access)
7. Walls R, Olivier G, Eksteen R (2017) Informal settlement fires in South Africa: Fire engineering overview and full-scale tests on ''shacks''. Fire Saf J 91:997–1006
8. Maranghides M, Mell W (2009) A case study of a community affected by the Witch and Guejito Fires, NIST Technical Note (NIST TN)—1635 https://doi.org/10.6028/NIST.TN.1635
9. Blanchi R, Leonard J (2005) Investigation of bushfire attack mechanisms resulting in house loss in the ACT Bushfire 2003. Bushfire CRC report
10. Suzuki S, Manzello SL (2018) Characteristics of firebrands collected from actual urban fires. Fire Technol 54:1533–1546
11. Manzello SL, Suzuki S, Gollner MJ, Fernandez-Pello AC (2020) The role of of firebrand combustion in large outdoor fire spread. Prog Energy Combust Sci 76:100801
12. Fernandez-Pello AC, Lautenberger C, Rich D, Zak C, Urban J, Hadden R, Scott S, Fereres S (2014) Spot fire ignition of natural fuel beds by hot metal particles, embers and sparks. Combust Sci Technol 187(1–2):269–295
13. Manzello SL, Cleary TG, Shields JR, Yang JC (2006) On the ignition of fuel beds by firebrands. Fire Mater 30:77–87
14. Tarifa CS, del Notario PP, Moreno FG (1965) On the flight paths and lifetimes of burning particles of wood. Proc Combust Inst 10:1021–1037
15. Lee S-L, Hellman JM (1969) Study of firebrand trajectories in a turbulent swirling natural convection plume. Combust Flame 13(6):645–655
16. Albini FA (1983) Transport of firebrands by line thermals. Combust Sci Technol 32(5–6):277–288

17. Ellis PF (2000) The aerodynamic and combustion characteristics of eucalypt bark—a firebrand study. Ph.D. thesis, Australian National University, Canberra, ACT
18. Koo E, Linn RR, Pagni PJ, Edminster CB (2012) Modelling firebrand transport in wildfires using HIGRAD/FIRETEC. Int J Wildl Fire 21:396–417
19. Tohidi A, Kaye NB (2017) Comprehensive wind tunnel experiments of lofting and downwind transport of non-combusting rod-like model firebrands during firebrand shower scenarios. Fire Saf J 90:95–111
20. Woycheese JP (2000) Brand lofting and propagation for large-scale fires. Ph.D. Thesis, University of California, Berkeley
21. Zhou K, Suzuki S, Manzello SL (2015) Experimental study of firebrand transport. Fire Technol 51:785–799
22. Muraszew A, Fedele JF (1976) Statistical model for spot fire spread. The Aerospace Corporation Report No. ATR-77758801, Los Angeles
23. Manzello SL, Cleary TG, Shields JR, Yang JC (2006) Ignition of vegetation and mulch by firebrands in Wildland/Urban Interface (WUI) fires. Int J Wildland Fire 15:427–431
24. Manzello SL, Cleary TG, Shields JR, Mell W, Yang JC (2008) Experimental investigation of firebrands: generation and ignition of fuel beds. Fire Saf J 43:226–233
25. Suzuki S, Manzello SL, Kagiya K, Suzuki J, Hayashi Y (2015) Ignition of mulch beds exposed to continuous wind driven firebrand showers. Fire Technol 51:905–922
26. Yin P, Liu N, Chen H, Lozano JS, Shan Y (2012) New correlation between ignition time and moisture content for pine needles attacked by firebrands. Fire Technol 50:79–91
27. Urban JL, Song J, Santamaria S, Fernandez-Pello C (2019) Ignition of a spot smolder in a moist fuel bed by a firebrand. Fire Saf J 108:102833
28. Cruz M et al (2015) A guide to rate of fire spread models for Australian vegetation. CSIRO Land and Water Flagship Canberra ACT and AFAC Melbourne, Vic
29. Suzuki S, Manzello SL (2017) Experiments to prove the scientific-basis for laboratory standard test methods for firebrand exposure. Fire Saf J 91:784–790
30. Santoso MA, Christensen EG, Yang J, Rein G (2019) Review of the transition from smouldering to flaming combustion in wildfires. Front Mech Eng 5:49. https://doi.org/10.3389/fmech.2019.00049
31. Manzello SL, Foote EID (2014) Characterizing firebrand exposure during wildland-urban interface fires: results of the 2007 Angora fire. Fire Technol 50:105–124
32. Manzello SL, Park SH, Cleary TG (2009) Investigation on the ability of glowing firebrands deposited within crevices to ignite common building materials. Fire Saf J 44:894–900
33. Kim DK, Sunderland P (2019) Fire ember pyrometry using a color camera. Fire Saf J 106:88–93
34. Urban JL, Vicariotto M, Dunn-Rankin D, Fernandez-Pello AC (2019) Temperature measurement of glowing embers with color pyrometry. Fire Technol 55(3):1013–1026
35. Ohlemiller T (1991) Smoldering combustion propagation on solid wood. Fire Saf Sci 3:565
36. Tse SD, Fernandez-Pello AC, Miyasaka K (1996) Controlling mechanisms in the transition from smoldering to flaming of flexible polyurethane foam. Proc Combust Inst 26:1505–1513
37. Aldushin AP, Bayliss A, Matkowsky BJ (2006) On the transition from smoldering to flaming. Combust Flame 145:579–606